Energy Spectrum of Atomic Electrons Ejected in Electron-Capture Decay of Fe^{55}†

J. G. PENGRA* AND B. CRASEMANN
Department of Physics, University of Oregon, Eugene, Oregon
(Received 9 May 1963)

The shape of the energy spectrum of orbital electrons ejected from Fe^{55} during nuclear decay by electron capture has been measured from 28 to 190 keV (the theoretical end point is at 218 keV). The electrons were detected in a proportional counter or in a semiconductor particle detector, in coincidence with Mn K x rays. The electron ejection probability decreases by a factor of 10^3 over the investigated energy range. The shape of the measured spectrum differs somewhat from theoretical predictions, in that the ejection probability falls off more slowly with energy. The discrepancy becomes more pronounced with decreasing energy. The contributions of L-electron ejection are considered.

I. INTRODUCTION

IN nuclear decay by orbital electron capture, atomic excitation and even ionization can occur due to the sudden change in nuclear charge. This paper is concerned with the process in which the balance of the disintegration energy is shared between the neutrino and an orbital electron that is ejected.

Primakoff and Porter have developed the theory of atomic excitation accompanying orbital electron capture.[1] Using the sudden perturbation approximation, they have derived expressions for $P_{(2)}$, the total probability per K-capture event that a double vacancy in the K shell is formed, as well as for P_{ejec}, the probability that the noncaptured K electron is ejected, and for the momentum spectrum of the ejected electrons. In calculating the transition-matrix elements, the initial electron space wave function is written as the product of two $1s$ wave functions, with the initial nuclear charge, Z_i, replaced by an effective charge, $(Z_i-\gamma_2)$, to take account of the extent to which one K electron shields the other from the nuclear Coulomb attraction. A factor $\exp(\gamma_1 r_{12}/a)$ is introduced to describe the effect of the electron-electron Coulomb interaction on their spatial correlation. As the final and initial electronic wave functions are nearly orthogonal, the transition-matrix elements depend sensitively on the quantity $(\gamma_1+\gamma_2)$, which is set equal to 0.5 in order to fit the variational nonrelativistic two-electron wave function given by Hylleraas.[2] The influence of the $L,M,\cdots$ electrons on the K electrons is neglected in writing the wave function. In the final result, the effect of occupied higher orbitals on the K-shell ionization probability is expressed by a somewhat uncertain correction factor.

Wolfsberg[3] has pointed out that the ejection of L electrons in K capture, and the ejection of K electrons accompanying L capture, can contribute significantly to the total orbital electron ejection probability.

Experimental studies of electron excitation accompanying orbital electron capture by nuclei can test the validity of the assumptions underlying the theory and, thus, offer an opportunity for probing K-electron wave functions for many-electron atoms.

The most precise determination of $P_{(2)}$ is due to Lark and Perlman,[4] who used a fast scintillation coincidence spectrometer to measure K x ray, K x-ray coincidences in the electron-capture decay of Cs^{131}, and, hence, obtained the probability for the production of an atom with a completely vacant K shell. The result, $(2.5\pm0.2)\times10^{-5}$ per K-capture event in Cs^{131}, is about one-half the value predicted by the Primakoff-Porter theory. Measurements of $P_{(2)}$ for Ar^{37} by Miskel and Perlman,[5] for Ge^{71} by Langevin,[6] and for Cs^{131} by Daniel, Schupp, and Jensen[7] also gave results which are in reasonable agreement with theory.

The spectrum of ejected orbital electrons has not yet been studied closely over a substantial energy range. Three observations have been published. Miskel and Perlman[5] measured the energy distribution of electrons ejected in the disintegration of Ar^{37} (decay energy 816 keV) with kinetic energy up to 4 keV. The data show fewer low-energy electrons than predicted by the Primakoff-Porter theory, and the number of observed electrons falls off more slowly with energy than predicted. The energy range studied comprises 73% of all ejected electrons, but constitutes only about 0.5% of the entire range over which these electrons are distributed.

Langevin's Ge^{71} electron spectrum[6] was obtained with a gaseous source in a proportional counter surrounded by an anticoincidence Geiger-counter shield. It can be compared with theory over a range from approximately 10 to 40 keV kinetic energy of the ejected electrons; the theoretical endpcint is at 212 keV. We find fair agreement of Langevin's data with the Primakoff-Porter theory; at low energies, the measured spectrum falls off more gradually with energy than the theoretical distribution. However, interpretation of the measured spectrum is complicated because it is produced by three different types of events: (1) a double K vacancy is filled and two K x rays are emitted which escape from

† Supported by the National Science Foundation.
* Present address: Whitman College, Walla Walla, Washington.
[1] H. Primakoff and F. T. Porter, Phys. Rev. **89**, 930 (1953).
[2] See H. A. Bethe and E. E. Salpeter, in *Handbuch der Physik*, edited by S. Flügge (Springer-Verlag, Berlin, 1957), Vol. 35, p. 232.
[3] M. Wolfsberg, Phys. Rev. **96**, 1712 (1954).
[4] N. L. Lark and M. L. Perlman, Phys. Rev. **120**, 536 (1960).
[5] J. A. Miskel and M. L. Perlman, Phys. Rev. **94**, 1683 (1954).
[6] M. Langevin, Compt. Rend. **245**, 664 (1957); J. Phys. Radium **19**, 34 (1958).
[7] H. Daniel, G. Schupp, and E. N. Jensen, Phys. Rev. **117**, 823 (1960).

the counter; in addition to energy released in filling the L shell, the energy of the ejected orbital electron alone is recorded; (2) the double K vacancy is filled under emission of one x-ray and one Auger electron; the x-ray escapes and the recorded energy includes that of the ejected orbital electron plus approximately 8 keV Auger-electron energy; (3) two Auger electrons are emitted, dissipating an additional 16 keV, approximately, in the counter. Furthermore, the contributions of L capture and L-electron ejection have not been considered in this work.

Daniel, Schupp, and Jensen[7] have measured the energy of electrons ejected in the decay of Cs^{131}, from 40 to 250 keV (endpoint 284 keV), using scintillation counters. The standard deviations are very large, and there is only approximate agreement with the theoretical spectrum.

II. EXPERIMENTAL REQUIREMENTS

Because of its low probability, orbital-electron ejection in electron capture can only be observed reliably in isotopes which decay purely by electron capture to the ground state of the daughter nucleus. Gamma transitions must be absent, since they would contribute conversion and Compton electrons, swamping the phenomenon under study. Similarly, beta-active contaminants would render the measurements unreliable.

It is advantageous to study an isotope of low atomic number Z, since the total probability for electron ejection[1] is approximately proportional to Z^{-2}. In addition, relativistic effects, neglected in the Primakoff-Porter theory, are less important at low Z.

Iron-55 fulfills these requirements. Oak Ridge National Laboratory produces this material by neutron capture of enriched Fe^{54}. The important contamination is 45-day Fe^{59}. By storage over a sufficiently long period, the Fe^{59} disintegration rate can be allowed to decay to a negligible level, as compared with the 2.7-yr Fe^{55} activity.

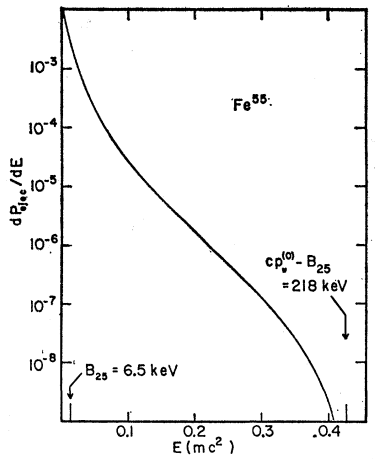

FIG. 1. Energy distribution of K electrons ejected in K capture of Fe^{55}, after the theory of Primakoff and Porter (Ref. 1). The ordinate represents the ejection probability per capture event per mc^2 energy interval. The K binding energy of manganese, B_{25}, and the theoretical end point of the ejected-electron spectrum at 218 keV are indicated.

The theoretical energy spectrum of K electrons ejected in K capture of Fe^{55} is represented in Fig. 1, which shows a logarithmic plot of $dP_{ejec}/dE = (1/\beta)dP_{ejec}/dp$. Here, p is the momentum of the ejected electron and E its kinetic energy (in units of mc and mc^2, respectively), $\beta = p/E = dp/dE$ is the ratio of electron speed to that of light, and dP_{ejec}/dp is the ejected-electron momentum distribution per K-capture event[1]:

$$\frac{dP_{ejec}}{dp} = \left[\frac{32(1-\gamma)^2}{\pi a^3 (Z_i-\gamma)^5}\left(\frac{mc^2}{cp_\nu^{(0)}}\right)^2 p^2\left(\frac{cp_\nu^{(0)}}{mc^2}-\frac{B_{Z_f}}{mc^2}-\frac{p^2}{2}\right)^2\left(\frac{2\pi\alpha Z_f}{\beta}\right)\left(\frac{1}{1-e^{-2\pi\alpha Z_f/\beta}}\right)\right] \times \frac{\exp\{-(4\pi\alpha Z_f/\beta)\tan^{-1}[p/\alpha(Z_i-\gamma)]\}}{\{1+[p/\alpha(Z_i-\gamma)]^2\}^4}. \quad (1)$$

The atomic number of the parent nucleus is $Z_i = 26$, and $Z_f = 25$ is that of the daughter nucleus. The sum of the correlation and shielding constants discussed above is $\gamma = \gamma_1 + \gamma_2$; this is set equal to 0.5. The Bohr radius is a, and α is the fine-structure constant. The function enclosed by the first square brackets represents the momentum distribution in an allowed β^--spectrum with end-point energy $cp_\nu^{(0)} - B_{Z_f}$, where $cp_\nu^{(0)}$ is the energy carried off by the neutrino in the absence of orbital electron excitation, and B_{Z_f} is the K-shell binding energy for atomic number Z_f. Taking 231 keV for the disintegration energy[8] of Fe^{55}, one obtains 224 keV for $cp_\nu^{(0)}$, and 218 keV for the end point of the ejected-electron spectrum. In the process, the energy taken up by the expansion of the electron cloud when Z decreases by one unit is approximately 5 keV.[9]

Figure 1 shows that the theoretical probability for electron ejection is small, and falls off steeply with increasing energy. By detecting the ejected electrons in coincidence with at least one Mn K x-ray signalling a capture event, background can be minimized. Furthermore, decays followed by double K Auger-electron emission are thus excluded from the measurements, reducing the energy uncertainty. Ideally, one might wish to select coincidences with double K x rays only, signaling the

[8] *Nuclear Data Sheets*, compiled by K. Way, *et al.* (Printing & Publishing Office, National Academy of Sciences–National Research Council, Washington 25, D. C.), NRC 59-2-9.

[9] P. Benoist-Gueutal, quoted in R. Bouchez and P. Depommier, Rept. Progr. Phys. **23**, 395 (1960).

filling of a completely vacant K shell by two radiative transitions. However, the counting rate would be very much reduced by this requirement, as can be seen from the following considerations. Let the K-shell fluorescent yield be denoted by ω_K, and let ϵ be the K x-ray detection efficiency (including solid angle). The probability that an entirely vacant K shell is filled by two radiative transitions ("process 1") is ω_K^2; the probability that both K x rays are detected is $\omega_K^2\epsilon^2$, and the probability that only one x ray is detected is given by $2\omega_K^2\epsilon(1-\epsilon)$. The probability that the vacant K shell is filled under emission of one K x ray and one K Auger electron ("process 2"), and that the x ray is detected, is $2\omega_K(1-\omega_K)\epsilon$. A third possible process consists in the emission of two K Auger electrons, with a probability $(1-\omega_K)^2$; in this case, of course, the probability of x-ray detection is zero. With $\omega_K=0.26$ for manganese,[10] the filling of a completely vacant K shell following Fe^{55} decay occurs by process 1 in 6.8% of all cases, by process 2 in 38.5%, and by process 3 in 54.7%. With an x-ray detection efficiency of 0.2, near the maximum attainable in our experiment for reasons of geometry, only approximately 3% of the detected x rays which signal the filling of a completely vacant K shell are double x rays. The x-ray detector was, therefore, set to accept single Mn K x rays, in order to avoid excessively long counting periods for accumulating statistically significant data at the higher energies. Even so, approximately 100 h of counting were required for each run.

III. APPARATUS AND PROCEDURES

A. Sources

Reactor-produced Fe^{55} for this experiment was purchased from the Oak Ridge National Laboratory and stored for 7 yr. During this storage time, shorter lived contaminants (especially beta-active 45-day Fe^{59}, $\leqslant 10\%$ of the activity at the time of production) decayed to a negligible level, compared with the 2.7-yr Fe^{55} activity ($<5\times10^{-18}$ Fe^{59} decays per Fe^{55} decay).

Sources were made by evaporating drops of $FeCl_3$ solution on 50-μg/cm^2 Formvar films, prepared according to the method of Bachman[11] and weighed. (The $FeCl_3$ solution was neutralized before preparing a source, presumably producing colloidal ferric hydroxide. This dried in a very uniform layer.) The source used for obtaining the data here reported had a strength of 800 dis/sec and was somewhat less than 40 μg/cm^2 thick.

B. Detectors

A proportional counter was employed as the electron detector in the energy range from 25 to 80 keV. Figure 2 shows a cross section of the counter, which was constructed of brass and provided with a 0.0036-in. stainless steel center wire. The source holder was mounted in the wall. Cathode continuity across the source window was maintained by a film of aluminized Mylar; without this provision, the irregular field configuration near the source caused an apparent energy shift. For maximum stability, a 3000-V dry-cell battery was used as the high-voltage supply for the counter. The counting gas was argon with a 4% CO_2 admixture.[12] The operating pressure was 3 atm. The gas from the supply cylinder was taken through a dry-ice cold trap and allowed to flow through the counter continuously at a rate of approximately 30 cm^3/min. The flow system gave excellent long-term stability.

For energies above 50 keV, an n-p junction detector with an active area of 0.4 cm^2 was used (Solid State Radiations, Inc., shallow phosphorus diffused detector Type NPSG-75). The detector and source assembly were mounted in a vacuum tank to reduce electron energy loss and scattering. A Mylar exit window was provided for the x-rays. With a charge-sensitive preamplifier after a design of Chase, Higinbotham, and Miller,[13] a line width of 13 keV was achieved. Preamplifier tube noise limited the use of this detector to electron energies above 50 keV.

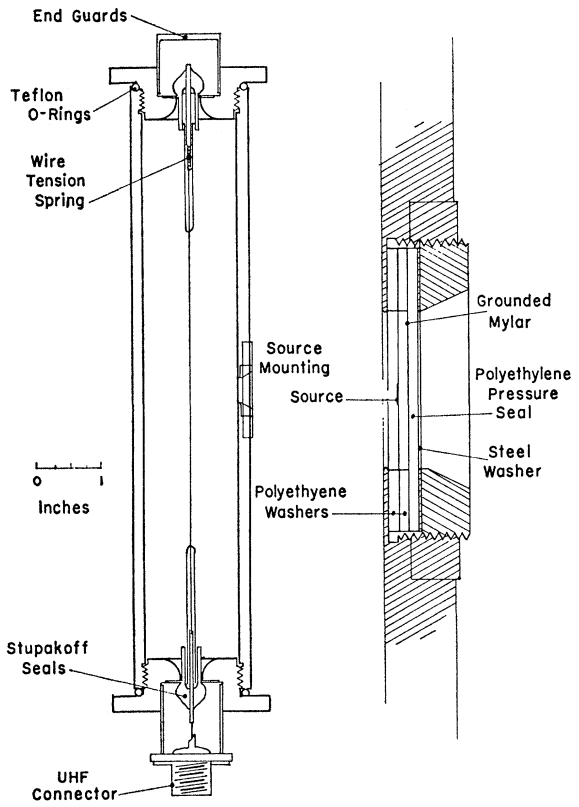

FIG. 2. Cross section of proportional counter and detail of source and window assembly.

[10] G. J. Nijgh, A. H. Wapstra, and R. Van Lieshout, in *Nuclear Spectroscopy Tables* (North-Holland Publishing Company, Amsterdam, 1959), Table 7.2-3.

[11] C. H. Bachman, *Techniques in Experimental Electronics* (John Wiley & Sons, Inc., New York, 1948), p. 238.

[12] Obtained commercially from Pacific Oxygen Company, Oakland, California.

[13] R. L. Chase, W. A. Higinbotham, and G. L. Miller, IRE Trans. Nucl. Sci. 8, 147 (1961).

The x rays were detected with a Harshaw NaI(Tl) crystal, coupled to a Du Mont 6292 photomultiplier tube. The crystal was covered with a 0.005-in. beryllium window. Figure 3 shows the manganese K x-ray spectrum obtained with this detector.

C. Electronics

The pulses from the last dynode of the x-ray detector photomultiplier were amplified in a Goldsworthy preamplifier, limited, and put into a Hamner Model 328 linear amplifier. The limiter was required to avoid overloading of the linear amplifier by large pulses due to background radiation.

The proportional-counter pulses were fed into a Radiation Counter Laboratories Model A1A preamplifier and then into a Baird-Atomic Model 215 nonoverloading linear amplifier, with a pulse clipping time of 1 μsec. The same linear amplifier was used with the solid state detector preamplifier.

The coincidence circuit consisted of a Baird-Atomic Model 502 4-channel coincidence analyzer that had been modified, separating it into two identical 2-channel units. The coincidence circuits were connected to the integral discriminator of the linear amplifier in the electron channel and to the differential discriminator in the x-ray channel (see block diagram, Fig. 4). The internal delay of approximately 1.6 μsec in the differential discriminator was compensated by a variable delay in the electron channel. This variable delay was also used to adjust the coincidence timing when the slower proportional counter was employed for electron detection.

A typical delay curve for the proportional-counter-scintillation-counter-system is shown in Fig. 5. A rather slow coincidence resolving time of 3 μsec was required because of the inherent variation of the proportional counter's response time, which shows itself in the width of the delay curve. Because of the very low counting rates in each channel, the long resolving time did not produce excessive chance coincidence counts. With the solid state counter, the coincidence resolving time was reduced to 1.5 μsec.

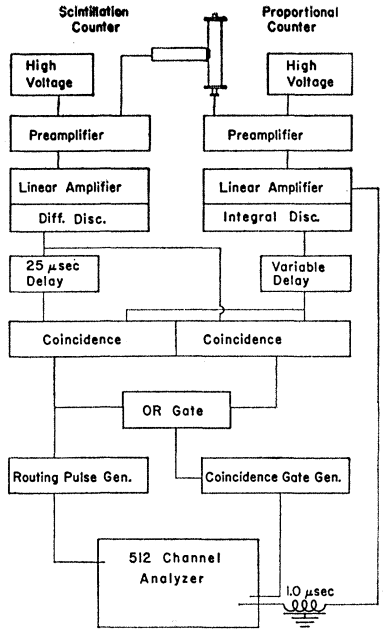

FIG. 4. Schematic diagram of coincidence spectrometer.

The output of the coincidence circuit triggered a Tektronix Model 163 waveform generator, which supplied a 5-μsec pulse for the coincidence gate of the Nuclear Data Series 120 multichannel analyzer. The output from the linear amplifier in the electron channel had to be delayed 1 μsec for proper overlap with the coincidence gate at the analyzer. This delay did not affect linearity.

The chance coincidence spectrum was measured simultaneously with the total spectrum. For this purpose, a second identical coincidence circuit was provided with the same input pulses as the first one, but with a 25-μsec delay in one channel. The output pulses from the two coincidence circuits triggered the Tektronix gate generator through an OR gate. In addition,

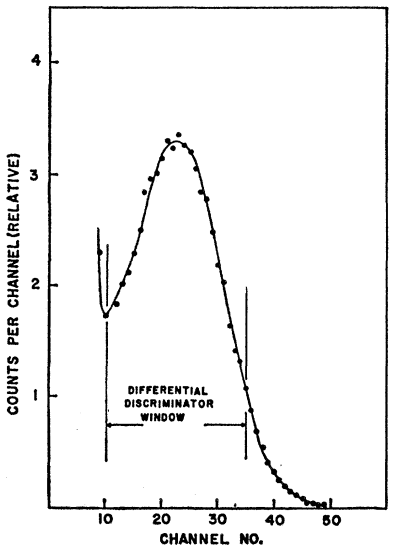

FIG. 3. Scintillation spectrum of Mn K x ray. The position of the discriminator window in the x-ray channel of the coincidence spectrometer is indicated.

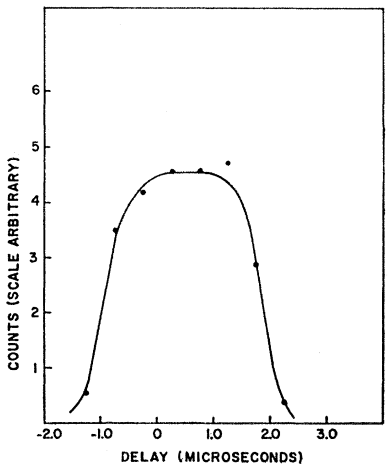

FIG. 5. X-ray–electron coincidence counting rate as a function of delay in the electron channel, employing the proportional counter.

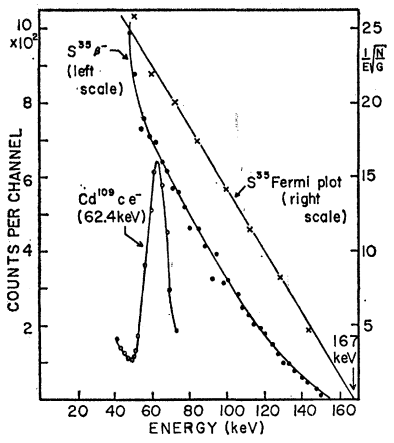

FIG. 6. Examples of semiconductor detector performance: Cadmium-109 conversion-electron peak (arbitrary scale on ordinate), continuous beta spectrum from S^{35}, and Fermi plot constructed from the latter.

the output of the second coincidence circuit triggered a univibrator that provided a routing pulse for the analyzer, causing the chance coincidence spectrum to be stored in one half of the analyzer memory, while the spectrum arriving without routing pulses (chance plus true) was stored in the other half of the memory. This system saved counting time and increased the reliability of the data.

D. Calibration

Conversion electron lines from Cd^{109}(62.4 keV) and Ce^{144}(91.4 keV) were used in the energy calibration of the proportional counter; in calibrating the solid state detector, the 329.9-keV line from I^{131} was used as well. The coincidence circuit timing was adjusted by measuring coincidences between conversion electrons and K x rays from the isomeric transition in the Ag^{109} daughter of Cd^{109}.

The linearity of the energy response of the solid-state detector was verified by measuring the continuous beta spectrum from S^{35} (end point 167 keV). The resultant Fermi plot is straight and shows the correct end point (Fig. 6).

IV. CORRECTIONS

The observed electron spectrum can be distorted due to the following causes: wall effect in the proportional counter, backscatter and self-absorption in the source, internal bremsstrahlung, energy shift due to coincident Auger electrons, and background. These effects are now discussed.

A. Wall Effect

Electrons that escape from the active volume of the proportional counter through the ends or by striking the walls dissipate less than their full energy in the gas. A computer program was written to estimate the resultant distortion of the spectrum. Simplifying assumptions, of opposite effect, were that (1) an electron which leaves the sensitive gas volume at a distance R from the source dissipates approximately as much energy in that volume as an electron of range R, and (2) backscattering into the sensitive volume can be neglected. The maximum distance from the source to the edge of the counting volume was divided into 70 equal intervals ΔR. For the average value of R in each interval, the Primakoff-Porter spectrum was cut off at the appropriate energy E_R, which is the energy of electrons with range R in the counter gas. The spectrum was integrated from E_R to the endpoint and the integrated number of counts, divided by the energy range ΔE_R corresponding to the range interval ΔR, was added to the spectrum at E_R. The contributions to the spectrum from each interval $(R,R+\Delta R)$ were summed, each weighted by the solid angle for which the distance from the source to the edge of the counting volume falls into this interval. Thus, the distortion that finite counter size would produce in a spectrum of the shape given by Primakoff and Porter[1] was computed. The observed spectrum was corrected accordingly. The correction does not exceed 7% in the electron-energy interval from 30 to 80 keV, but increases rapidly at higher energies. The proportional counter was, therefore, not employed above 80 keV.

B. Scattering in Source and Backing

The range of backscattered electrons is approximately one-half their original range.[14] Electrons from the source that are backscattered into the counter are, therefore, added to the observed spectrum at a lower energy. For example, backscattered 40-keV electrons appear with 28 keV, and 50-keV electrons are backscattered with 34 keV. Because the intensity of the ejected-electron spectrum falls off very rapidly with energy, backscattered electrons *add* a relatively small fraction to the spectrum, even at the lowest energy: The 50-μg/cm^2 Formvar backing will add 2% to the spectrum at 30 keV, 1% at 40 keV, and only 0.1% at 80 keV. Saturation backscattering from the Mylar and polyethylene pressure seal will add less than 6, 5, and 2%, respectively, at these three energies. At the same time, electrons originating beneath the surface of the 40-μg/cm^2 source layer can be backscattered by the source material, so that they are not counted. This process *subtracts* an estimated 10% from the observed spectrum at 30 keV, 6% at 40 keV, and 2% at 80 keV.[15] The net effect of backscattering is, therefore, negligible compared with the statistical counting errors.

Small-angle scattering within the source will cause some energy degradation, resulting in a slight excess of low-energy counts. While this effect is difficult to estimate quantitatively, it is regarded as negligible because of the shape of the spectrum and the thinness of the source.

---

[14] G. Fournier, as quoted in G. J. Nijgh, A. H. Wapstra, and R. Van Lieshout, in *Nuclear Spectroscopy Tables* (North-Holland Publishing Company, Amsterdam, 1959), p. 42.

[15] Backscattering estimates have been calculated from the formulas of Seliger, quoted in G. J. Nijgh A. H. Wapstra, and R. Van Lieshout, in *Nuclear Spectroscopy Tables* (North-Holland Publishing Company, Amsterdam, 1959), Sec. 5.1.

C. Internal Bremsstrahlung

The spectrum of internal bremsstrahlung emitted by Fe^{55} in coincidence with Mn K x rays has recently been measured by Biavati *et al.*[16] and found to be in agreement with Martin and Glauber's theory[17] for radiative $1S$ electron capture. The expected counting rate in our experiment, due to internal bremsstrahlung quanta in coincidence with K x rays, was calculated from the theoretical spectrum of Martin and Glauber, taking into account the appropriate photon detection efficiency.

The photon efficiency of the proportional counter was calculated from tabulated absorption coefficients[18] and the average path length in the counter. The effect of internal bremsstrahlung photons on the semiconductor detector was calculated by using the photoelectric and Compton cross sections for silicon[18] and considering that photons, to be counted, must interact with the material in the depletion layer, of thickness $(\rho V)^{1/2}/3\ \mu$ (ρ is the resistivity in Ω-cm, and V is the applied reverse bias voltage).[19] Experiments on the response of the semiconductor detector to photons in this energy range show that the efficiency calculated in this manner is approximately correct, but may be slightly high.[20]

The relative contribution of internal bremsstrahlung to the observed spectrum was calculated on the assumptions that the ejected-electron spectrum is nearly that given by Primakoff and Porter,[1] that photons detected with the proportional counter are registered at their full energy, and that photons detected with the solid-state counter are registered with their full energy if they appear in the photopeak, but are registered with equal likelihood at any energy up to the Compton edge if they appear in the Compton distribution. It was taken into account that the probability for an ejected electron to be accompanied by an observed single K x ray is approximately twice the probability for an internal bremsstrahlung photon to be accompanied by such an x ray, where the ratio of these probabilities is

$$[2\omega_K{}^2\epsilon(1-\epsilon)+2\omega_K(1-\omega_K)\epsilon]/\omega_K\epsilon.$$

(The notation has been defined in Sec. II, above.) Hence, an internal bremsstrahlung correction factor as a function of energy was obtained and applied to the observed spectrum. Internal bremsstrahlung contributes from 1% of the total counting rate at 30 keV to 10% at 80 keV in the proportional counter, and from 2% at 50 keV to 10% at 200 keV in the semiconductor detector.

D. Auger Electrons and Background

When a double K-shell vacancy is created by K capture and K-electron ejection, one vacancy must be filled through a radiative transition, in order to fulfill the coincidence requirement of the counting apparatus. If the x ray or Auger electron emitted when the second vacancy is filled enters the electron detector, then their energy can be summed with that of the ejected orbital electron. Through this effect, an energy of approximately 2.7 keV, on the average, is added to that of each ejected orbital electron detected in the proportional counter. Due to the smaller solid angle subtended by the solid state counter, the average energy added in this detector is 1.4 keV. The energy scale of the measured spectrum was adjusted accordingly, and the ensuing uncertainty was included in the probable errors given for the energy.

Background radiation producing coincidences between the x-ray and electron detector signals added a small number of counts to the measured spectrum. The spectrometer was operated without source for suitable intervals to determine the background spectrum, which was subtracted from the data.

V. EXPERIMENTAL RESULTS AND DISCUSSION

A. Ejected-Electron Spectrum

The experimentally determined shape of the Fe^{55} ejected-electron spectrum is shown in Fig. 7. The data have been corrected as described in the preceding sections. For comparison, the energy spectrum of ejected K electrons predicted by the Primakoff-Porter theory[1] is also shown. The data have been arbitrarily normalized to the theoretical curve in the high-energy region, by employing a construction[1] that is analogous to the Fermi plot for beta spectra, and yields a straight line intercepting the energy axis at 218 keV.

It is apparent that the slope of the measured spectrum differs markedly from that of the theoretical curve, and that this discrepancy increases with decreasing energy. This trend, consisting of a slower variation of ejected-electron intensity with energy than predicted, is also exhibited by the results of Miskel and Perlman[5] for A^{37}, and is not inconsistent with the data of Daniel, Schupp, and Jensen[7] for Cs^{131}.

B. L-Shell Contributions

The possibility that L capture and L-electron ejection could account in part for the observed shape of the ejected-electron spectrum must be examined. Following the suggestion of Wolfsberg,[3] an expression for the probability of L-electron ejection was obtained by suitable modification of the theory of Levinger[21] for L-electron excitation accompanying ordinary beta decay. Levinger's computation is based on expanding the initial-state electronic wave function in terms of final-state wave functions, so that the coefficient of the positive-energy final-state wave function represents the relative probability amplitude for finding the electron ejected after the nuclear charge has suddenly changed. The result was modified by introducing a factor that, in

[16] M. H. Biavati, S. J. Nassiff, and C. S. Wu, Phys. Rev. **125**, 1364 (1962).
[17] P. C. Martin and R. J. Glauber, Phys. Rev. **109**, 1307 (1958).
[18] C. M. Davisson, in *Beta- and Gamma-Ray Spectroscopy*, edited by K. Siegbahn (North-Holland Publishing Company, Amsterdam, 1955), Appendix I.
[19] S. S. Friedland and F. P. Ziemba, in *Methods of Experimental Physics*, edited by L. C. L. Yuan and C.-S. Wu (Academic Press, Inc., New York, 1961), Vol. 5, p. 267.
[20] Experiments conducted in collaboration with D. O. Wells.
[21] J. S. Levinger, Phys. Rev. **90**, 11 (1953).

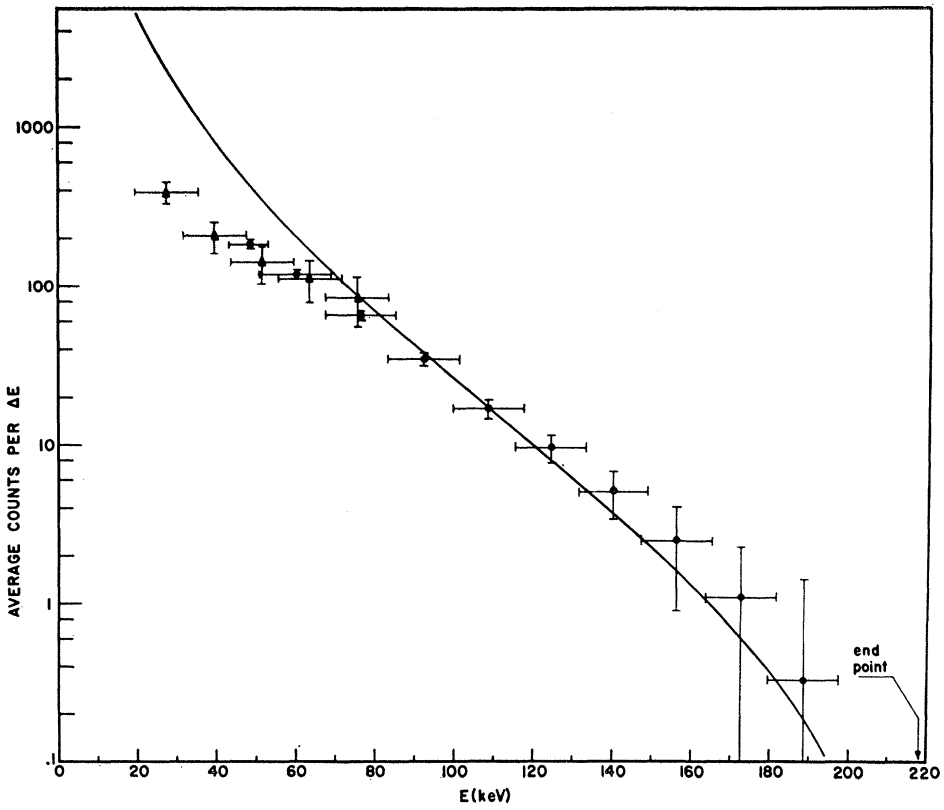

FIG. 7. Measured energy spectrum of orbital electrons ejected in electron-capture decay of Fe^{55}. The ordinate scale, showing counts per channel, is arbitrary. Triangles represent measurements with the proportional counter; the remaining points have been obtained with the solid state detector. The shape of the theoretical spectrum (Ref. 1) of K electrons ejected in K capture is indicated for comparison (solid curve). The theoretical end point is at 218 keV.

Primakoff and Porter's theory, arises from the nuclear part of the Hamiltonian, viz., $E_{\max}{}^{-2}(E_{\max}-E)^2$. Furthermore, Levinger's result for beta decay (with a change $\Delta Z=1$ in effective nuclear charge) was multiplied by $(\Delta Z)^2=0.0225$, to take into account the smaller change in nuclear charge "seen" by an L electron when K capture takes place, resulting in a proportionately smaller perturbing potential.[3] The value $\Delta Z=0.15$ follows from Slater's recipe[22] for estimating shielding constants. The results of the calculation are represented in Fig. 8. Only at very low energies does ejection from the L shells contribute significantly to the total ejection probability. In the energy range covered by the present experiments, the K/L ejection ratio is of the order of 10^3, i.e., due to shielding, L ejection does not contribute appreciably to the spectrum at these energies.

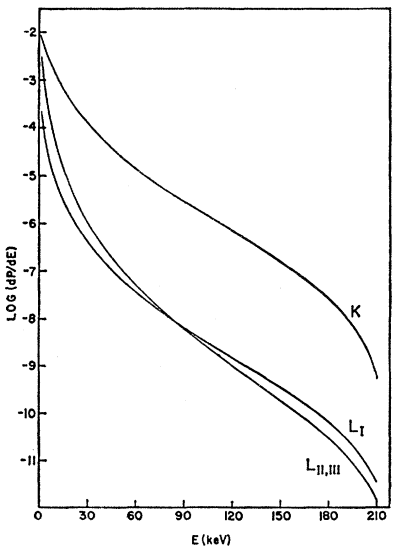

FIG. 8. Energy spectra of K, L_{I}, and $L_{\mathrm{II}}+L_{\mathrm{III}}$ electrons ejected in K-capture decay of Fe^{55}, after the theory of Levinger (Ref. 21), modified as indicated in the text. The ejection probability dP/dE is per capture event per mc^2 energy interval.

Electron ejection accompanying L capture (rather than K capture) does not lead to a spectrum with a shape that is materially different from that given by Primakoff and Porter,[1] as can be seen most readily from Levinger's *ansatz*.[21]

In order to bring the theoretical spectrum shape into agreement with the measured results, it may be necessary to modify the form of the initial-state K-electron wave function to take more detailed account of shielding and electron-electron correlations.

ACKNOWLEDGMENTS

We wish to thank D. O. Wells, H. W. Lefevre, and J. L. Powell for many helpful discussions, and the University of Oregon Statistical Laboratory and Computing Center for computer time.

[22] J. C. Slater, Phys. Rev. **36**, 57 (1930).